Onsager coefficients for systems with periodic potentials

Alexandre Rosas, Christian Van den Broeck, and Katja Lindenberg

Onsager coefficients for systems with periodic potentials

Alexandre Rosas*
*Departamento de Física, CCEN, Universidade Federal da Paraíba,
Caixa Postal 5008, 58059-900, João Pessoa, Brazil.*

Christian Van den Broeck
Hassel University, B-3590 Diepenbeek, Belgium.

Katja Lindenberg
*Department of Chemistry and Biochemistry, and BioCircuits Institute,
University of California San Diego, La Jolla, California 92093-0340, USA.*

We carry out the thermodynamic analysis of a Markovian stochastic engine, driven by a spatially and temporally periodic modulation in a d-dimensional space. We derive the analytic expressions for the Onsager coefficients characterizing the linear response regime for the isothermal transfer of one type of work (a driver) to another (a load), mediated by a stochastic time-periodic machine. As an illustration, we obtain the explicit results for a Markovian kangaroo process coupling two orthogonal directions, and find extremely good agreement with numerical simulations. In addition, we obtain and discuss expressions for the entropy production, power and efficiency for the kangaroo process.

I. INTRODUCTION

The evaluation of Onsager coefficients for machines operating under the influence of time-periodic perturbations is a recent development [1–12]. In a recent paper [13] we obtained Onsager coefficients for a one-dimensional system composed of a Brownian particle under the influence of a background time-independent periodic potential perturbed by modulated periodic potentials (both in time and space) and in contact with a heat bath at temperature T. By separating the modulating potential into two parts, a driving contribution which exerts work on the Brownian particle and a load on which the Brownian particle exerts work, we showed that the Brownian particle could mediate the work transfer.

Here, we generalize our results on two fronts. First, instead of only diffusive processes, we allow the underlying dynamics of the particle to be a general Markov process obeying detailed balance. Second, we extend the results to higher dimensions. This is particularly interesting because it allows us to consider the problem of work transfer between different degrees of freedom with a coupling mediated by a microscopic machine. The simplest concrete example are forces operating on a Brownian particle in spatially orthogonal directions, in presence of a substrate potential. Even though we have an explicit and exact result for the Onsager coefficients, it is expressed in terms of the eigenfunctions and eigenvalues of the stochastic motion in the space-periodic substrate potential, which are typically not known for non-trivial potentials [14]. The fact that our result are valid for any Markov process, allows to consider coupling via a so-called "kangaroo process" [15], in which the particles hop rather than diffuse in the substrate potential. Besides the explicit expression for the Onsager coefficients, the discovery of this exactly solvable model is another main contribution of the present paper.

The outline of the rest of this paper is as follows. In Sec. II we describe the set-up of the problem of periodic Markovian dynamics. Section III connects the Markovian dynamics with the thermodynamics and presents the definition of several quantities that will be used throughout the paper. Next, Sec. IV presents our results for the Onsager coefficients. Sections V and VI present our results for the kangaroo process as an example of an exactly solvable model for which we are able to calculate explicit expressions for the Onsager coefficients (Section V) and for several quantities of interest, namely entropy production, power and efficiency (Section VI). Finally, we summarize our results in Section VII.

II. PERIODIC MARKOVIAN DYNAMICS

Our starting point is the Markovian evolution equation for the probability density $\mathcal{P}_u(\boldsymbol{x}, t)$ to observe the system (e.g., a Brownian particle), at "location" $\boldsymbol{x}$:

$$\frac{\partial \mathcal{P}_u(\boldsymbol{x}, t)}{\partial t} = \hat{W}(\boldsymbol{x}, t)\mathcal{P}_u(\boldsymbol{x}, t). \tag{1}$$

While we refer, for conceptual simplicity, to $\boldsymbol{x}$ as "spatial location", this vectorial quantity can have a different interpretation with components not referring to degrees of freedom in translational space (i.e. a chemical coordinate, a rotational coordinate, a configurational state, etc.) The evolution operator $\hat{W}(\boldsymbol{x}, t)$ is both temporally periodic (with period τ) and spatially periodic [with period $\boldsymbol{L} = (L_1, L_2, \ldots L_d)$]. d is the dimensionality of the system, and L_l is the spatial period of the construction

* arosas@fisica.ufpb.br

in direction l. In the absence of time-modulated driving, the operator reduces to a time-independent spatially periodic form $\hat{W}_0(\boldsymbol{x})$. In view of the spatial periodicity, it will be convenient to consider, instead of the probability density $\mathcal{P}_u$ in unbounded space, the reduced probability density:

$$P(\boldsymbol{x}, t) = \sum_{k_1, k_2, \ldots, k_d = -\infty}^{\infty} \mathcal{P}_u(\boldsymbol{x} + \sum_{l=0}^{d} k_l L_l \hat{e}_l, t), \quad (2)$$

where $\hat{e}_l$ is a unit vector in direction l. $P(\boldsymbol{x}, t)$ obeys the master equation Eq. (1) in the region $[\boldsymbol{0}, \boldsymbol{L}]$ with periodic boundary conditions. From here on we drop the term "reduced" and simply refer to $P(\boldsymbol{x}, t)$ as the probability density. Because of the temporal periodicity of the potential this density function will, at long times, reach a periodic steady state, following the periodicity of $\hat{W}(\boldsymbol{x}, t)$. More precisely, the probability density at each point $\boldsymbol{x}$ returns to the same value after every period. The existence, uniqueness and convergence to this periodic state derives from the Perron Frobenius theorem (assuming ergodicity), see for example [16].

III. HEAT POWER AND ENTROPY PRODUCTION

To make the connection with thermodynamics, we introduce the adiabatic probability density $P_{\text{ad}}(\boldsymbol{x}, t)$. It is loosely speaking the "instantaneous" steady state distribution, achieved when the time-perturbation is infinitely slow. As we will see below, it naturally appears in the linear response analysis, even though we will be making no assumptions on the time scale. It is defined as the (normalized) zero eigenvector of the instantaneous Markov operator:

$$\hat{W}(\boldsymbol{x}, t) P_{\text{ad}}(\boldsymbol{x}, t) = 0. \quad (3)$$

In the absence of the temporal modulation, $P_{\text{ad}}(\boldsymbol{x}, t)$ reduces to the equilibrium probability density $P_{\text{eq}}(\boldsymbol{x})$, defined by the condition

$$\hat{W}_0(\boldsymbol{x}) P_{\text{eq}}(\boldsymbol{x}) = 0. \quad (4)$$

We now specify that the Markov process describes a modulated system in contact with a single heat bath. The adiabatic distribution $P_{\text{ad}}(\boldsymbol{x}, t)$ has to be identified with the canonical distribution, featuring the system's energy $U(\boldsymbol{x}, t)$:

$$P_{\text{ad}}(\boldsymbol{x}, t) = \frac{e^{-\beta U(\boldsymbol{x}, t)}}{Z_t}. \quad (5)$$

Here $\beta = (k_B T)^{-1}$, k_B is the Boltzmann constant, T is the temperature of the heat bath, and

$$Z_t = \int_0^{\boldsymbol{L}} e^{-\beta U(\boldsymbol{x}, t)} d\boldsymbol{x} \quad (6)$$

is the "partition function" at time t. The modulation is produced by two work sources 1 and 2 that shift the energy levels of the system according to the following prescription:

$$U(\boldsymbol{x}, t) = U_0(\boldsymbol{x}) + Y_1(\boldsymbol{x})\mathcal{F}_1(t) + Y_2(\boldsymbol{x})\mathcal{F}_2(t). \quad (7)$$

$U_0(\boldsymbol{x})$ is a time-independent background potential, and the functions $Y_j(\boldsymbol{x})$ are $\boldsymbol{L}$-periodic, while the $\mathcal{F}_j(t)$ have period τ. Henceforth the indices j and k (that will appear later) can take on the value 1 or 2. We consider a separate contribution of two periodic potentials $U_j(\boldsymbol{x}, t) = Y_j(\boldsymbol{x})\mathcal{F}_j(t)$ because this allows us to interpret the set-up as a thermodynamic machine that transforms work into work: the indices 1 and 2 refer to two work contributions with 1 playing the role of the load, i.e., the output work, and 2 the role of the driver, i.e., the input work. Such work to work transformations are frequently encountered in biological systems, one example being the the role of adenosine phosphate as an energy converter in the cell [17]. It is convenient to suppose that the amplitudes $\mathcal{F}_j(t)$ have the units of force and hence $Y_j(\boldsymbol{x})$ the units of length.

Due to conservation of total energy, the difference between the work done on the particle and the work done by the particle as a result of the interplay of the two potentials $U_1(x_1, t)$ and $U_2(x_2, t)$ is completely transformed into heat. More precisely, the first law can be written as follows [21]:

$$\frac{dU(\boldsymbol{x}, t)}{dt} = \frac{\partial U(\boldsymbol{x}, t)}{\partial t} + \nabla U(\boldsymbol{x}, t) \cdot \boldsymbol{v}, \quad (8)$$

where $\boldsymbol{v}$ is the velocity of the particle. $-\nabla U(\boldsymbol{x}, t) \cdot \boldsymbol{v}$ is the heat per unit time dissipated in the heat bath, and $\partial_t U(\boldsymbol{x}, t)$ the power driving the particle.

To formulate a steady state thermodynamic analysis, we obviously focus on the long time regime in which the stochastic dynamics of the systems becomes periodic, and consider quantities averaged over one period. Due to the periodicity, the average energy of the system is unchanged after each period, hence power is equal to heat, when averaged over one period. For the same reason, the entropy of the system returns to the same value after each period, and hence the entropy change per period in the entire construction is the average heat divided by the temperature. Combining both observations, we can write the entropy production rate averaged over one cycle as follows:

$$\dot{S} = \frac{1}{T} \frac{1}{\tau} \int_0^\tau \int_0^{\boldsymbol{L}} \frac{\partial U(\boldsymbol{x}, t)}{\partial t} P(\boldsymbol{x}, t) d\boldsymbol{x} dt. \quad (9)$$

The time periodicity of the forces suggests that a natural way to proceed is to expand $\mathcal{F}_j(t)$ in a Fourier series,

$$\mathcal{F}_j(t) = \sum_\mu F_\mu^{(j)} g_\mu(t), \quad (10)$$

where we have introduced the compact notation $\mu = (n, \zeta)$, $n = 1, 2, \ldots$, representing the Fourier modes, and

$\zeta = c$ or s such that

$$g_{n,c}(t) = \cos \omega_n t, \qquad g_{n,s}(t) = \sin \omega_n t, \qquad \omega_n \equiv \frac{2\pi n}{\tau}. \tag{11}$$

The $n = 0$ term can be absorbed into the background potential, so we need not consider it here. Using the Fourier expansion Eq. (10) in Eq. (9), we can write the entropy production in the standard form of irreversible thermodynamics [22]

$$\dot{S} = \sum_\mu \frac{1}{T} \frac{1}{\tau} \int_0^\tau \int_0^{\boldsymbol{L}} Y_1(\boldsymbol{x}) F_\mu^{(1)} \dot{g}_\mu(t) P(\boldsymbol{x},t) d\boldsymbol{x} dt + \sum_\mu \frac{1}{T} \frac{1}{\tau} \int_0^\tau \int_0^{\boldsymbol{L}} Y_2(\boldsymbol{x}) F_\mu^{(2)} \dot{g}_\mu(t) P(\boldsymbol{x},t) d\boldsymbol{x} dt \tag{12}$$

$$= \sum_\mu \left(X_\mu^{(1)} J_\mu^{(1)} + X_\mu^{(2)} J_\mu^{(2)} \right),$$

where we have introduced the thermodynamic forces (with usual unit of force over temperature) [11–13]:

$$X_\mu^{(j)} = \frac{F_\mu^{(j)}}{T}, \tag{13}$$

and the corresponding fluxes (with appropriate unit of speed):

$$J_\mu^{(j)} = \frac{1}{\tau} \int_0^\tau \int_0^{\boldsymbol{L}} Y_j(\boldsymbol{x}) \dot{g}_\mu(t) P(\boldsymbol{x},t) d\boldsymbol{x} dt. \tag{14}$$

IV. LINEAR IRREVERSIBLE THERMODYNAMICS AND ONSAGER COEFFICIENTS

So far, our results are valid for forces of any magnitude. To make further analytic progress, we turn to the regime of linear irreversible thermodynamics. We thus assume that the applied forces are sufficiently small, so that the fluxes (which vanish in the absence of forces) depend linearly on the forces:

$$J_\mu^{(j)} = \sum_{\nu,k} L_{\mu,\nu}^{j,k} X_\nu^{(k)}. \tag{15}$$

The proportionality constants $L_{\mu,\nu}^{j,k}$ are the celebrated Onsager coefficients, but introduced here in the novel context of Markov process periodically perturbed in space and time. They can obviously be calculated as follows:

$$L_{\mu,\nu}^{j,k} = \left. \frac{\partial J_\mu^{(j)}}{\partial X_\nu^{(k)}} \right|_{\mathbf{F}=\mathbf{0}}, \tag{16}$$

where $\mathbf{F} = \mathbf{0}$ means that all the $F_\mu^{(j)}$ are zero. The only dependence of $J_\mu^{(j)}$ on $X_\nu^{(k)}$ is through the probability density $P(\boldsymbol{x},t)$ [cf. Eq. (14)],

$$\frac{\partial J_\mu^{(j)}}{\partial X_\nu^{(k)}} = \frac{1}{\tau} \int_0^\tau \int_0^{\boldsymbol{L}} Y_j(\boldsymbol{x}) \dot{g}_\mu(t) \frac{\partial P(\boldsymbol{x},t)}{\partial X_\nu^{(k)}} d\boldsymbol{x} dt. \tag{17}$$

For the long time regime, the derivative of the master equation Eq. (1) with respect to $X_\nu^{(k)}$, at $\mathbf{F} = \mathbf{0}$, in the linear regime, can be written as

$$\frac{\partial P^{(\nu,k)}(\boldsymbol{x},t)}{\partial t} = \hat{W}^{(\nu,k)}(\boldsymbol{x},t) P_{\text{eq}}(\boldsymbol{x}) + \hat{W}_0(\boldsymbol{x}) P^{(\nu,k)}(\boldsymbol{x},t), \tag{18}$$

where

$$P^{(\nu,k)}(\boldsymbol{x},t) = \left. \frac{\partial P(\boldsymbol{x},t)}{\partial X_\nu^{(k)}} \right|_{\mathbf{F}=\mathbf{0}}, \tag{19}$$

$$\hat{W}^{(\nu,k)}(\boldsymbol{x},t) = \left. \frac{\partial \hat{W}(\boldsymbol{x},t)}{\partial X_\nu^{(k)}} \right|_{\mathbf{F}=\mathbf{0}}. \tag{20}$$

The solution of Eq. (18) is

$$P^{(\nu,k)}(\boldsymbol{x},t) = e^{\hat{W}_0(\boldsymbol{x})t} P^{(\nu,k)}(\boldsymbol{x},0)$$
$$+ \int_0^t dt' e^{\hat{W}_0(\boldsymbol{x})(t-t')} \hat{W}^{(\nu,k)}(\boldsymbol{x},t') P_{\text{eq}}(\boldsymbol{x}). \tag{21}$$

The first term on the right hand side vanishes because, in the long time regime, all information about the initial state is lost. Now, defining $t'' = t - t'$ and changing variables from t' to t'' in the remaining term of Eq. (21), we have

$$P^{(\nu,k)}(\boldsymbol{x},t) = \int_0^t dt'' e^{\hat{W}_0(\boldsymbol{x})t''} \hat{W}^{(\nu,k)}(\boldsymbol{x},t-t'') P_{\text{eq}}(\boldsymbol{x}). \tag{22}$$

We have thus introduced and defined all the quantities needed to calculate the Onsager coefficients. The calculation is somewhat lengthy and would distract from the results we wish to display, so we have placed the calculation in the Appendix and here just quote what is in fact the principal result of our paper:

$$L^{j,k}_{(m,\zeta),(n,\zeta')} = -(-1)^{\delta_{\zeta,c}}k_B^{-1}\frac{\omega_n}{2}\overline{[Y_j - \overline{Y_j}][Y_k - \overline{Y_k}]}(1-\delta_{\zeta,\zeta'})\delta_{m,n} + k_B^{-1}\sum_p \frac{1}{2}\frac{\omega_n^2\left[-\lambda_p\delta_{\zeta,\zeta'} + (-1)^{\delta_{\zeta,c}}\omega_n(1-\delta_{\zeta,\zeta'})\right]}{\omega_n^2 + \lambda_p^2}$$

$$\times \left[\int_0^{\boldsymbol{L}}\left[Y_j(\boldsymbol{x}) - \overline{Y_j}\right]\psi_p(\boldsymbol{x})d\boldsymbol{x}\int_0^{\boldsymbol{L}}\left[Y_k(\boldsymbol{x}') - \overline{Y_k}\right]\psi_p(\boldsymbol{x}')d\boldsymbol{x}'\right]\delta_{m,n}, \tag{23}$$

where $\delta_{\zeta,\zeta'}$ is the Kronecker delta, $|\psi_p\rangle$ is an eigenvector of $\hat{W}_0(\boldsymbol{x})$ with eigenvalue λ_p,

$$\hat{W}_0|\psi_p\rangle = \lambda_p|\psi_p\rangle, \tag{24}$$

and we have defined the average of a function $f(\boldsymbol{x})$ over the equilibrium distribution function as

$$\overline{f} = \int_0^{\boldsymbol{L}} P_{\mathrm{eq}}(\boldsymbol{x})f(\boldsymbol{x})d\boldsymbol{x}. \tag{25}$$

On the way to obtaining Eq. (23), we also used the following inner product of two (real) functions for (periodic) stochastic systems:

$$\langle f|g\rangle = \int_0^{\boldsymbol{L}}\frac{f(x)g(x)}{P_{\mathrm{eq}}(x)}d\boldsymbol{x}. \tag{26}$$

As the system returns to thermodynamic equilibrium in the absence of driving, the operator $\hat{W}_0$ must obey detailed balance. It is thus symmetric with respect to the above defined inner product. Hence the eigenvalues λ_p are real and one can choose corresponding real eigenfunctions $\psi_p(\boldsymbol{x})$. Furthermore, we assume that the latter form a complete set, so that $\sum_{p\geq 0}|\psi_p\rangle\langle\psi_p|$ is the unit operator.

We conclude this section by pointing out some general features and properties of our principal result Eq. (23). The Onsager matrix is positive, in agreement with the positivity of the entropy production. In particular all the diagonal Onsager coefficients are positive. The Onsager coefficients satisfy a frequency Curie principle since perturbations of different frequencies do no couple, cf. the overall factor in $\delta_{m,n}$. The Curie principle states that Onsager coefficients coupling processes of different symmetry character (for example scalar and vector) must be zero [23]. Here it refers to processes of different frequency that do not couple. We identify a symmetric contribution, proportional to $\delta_{\zeta,\zeta'}$ and anti-symmetric one in $1 - \delta_{\zeta,\zeta'}$. The latter does not contribute to the entropy production. Finally, for one-dimensional systems, Eq. (23) for the Onsager coefficients becomes

$$L^{j,k}_{(m,\zeta),(n,\zeta')} = -(-1)^{\delta_{\zeta,c}}k_B^{-1}\frac{\omega_n}{2}\overline{[Y_j - \overline{Y_j}][Y_k - \overline{Y_k}]}(1-\delta_{\zeta,\zeta'})\delta_{m,n}$$

$$+ k_B^{-1}\sum_p \frac{1}{2}\frac{\omega_n^2\left[-\lambda_p\delta_{\zeta,\zeta'} + (-1)^{\delta_{\zeta,c}}\omega_n(1-\delta_{\zeta,\zeta'})\right]}{\omega_n^2 + \lambda_p^2}\left[\int_0^L\left[Y_j(x) - \overline{Y_j}\right]\psi_p(x)dx\int_0^L\left[Y_k(x') - \overline{Y_k}\right]\psi_p(x)dx'\right]\delta_{m,n}. \tag{27}$$

This expression was first obtained in [13] for a Brownian particle in contact with a heat bath and under the influence of a spatially and temporally periodic potential in the overdamped limit. Here we have shown that this result is still valid for more general Markov processes. Obviously, the eigenfunctions of $\hat{W}_0$ and the specific functional dependence of the displacement functions $Y_j(x)$, which determine the eigenvalues and spatial averages, do depend on the particular Markov process, and so do the values of the Onsager coefficients. Nevertheless, formally the expression is the same.

V. KANGAROO PROCESS: AN EXACTLY SOLVABLE TWO-DIMENSIONAL MODEL

We are particularly interested in the Onsager coefficients linking "orthogonal" forces. By orthogonality we mean that the forces act in different subspace, i.e., one has $Y_j(\boldsymbol{x}) = Y_j(x_j)$ meaning that the perturbation j only acts along the coordinate x_j. The Onsager coefficients are then given by:

$$L^{j,k}_{(m,\zeta),(n,\zeta')} = -(-1)^{\delta_{\zeta,c}} k_B^{-1} \frac{\omega_n}{2} \overline{[Y_j - \overline{Y_j}]} \, \overline{[Y_k - \overline{Y_k}]} (1 - \delta_{\zeta,\zeta'})\delta_{m,n} + k_B^{-1}\sum_p \frac{1}{2}\frac{\omega_n^2 \left[-\lambda_p \delta_{\zeta,\zeta'} + (-1)^{\delta_{\zeta,c}}\omega_n(1-\delta_{\zeta,\zeta'})\right]}{\omega_n^2 + \lambda_p^2}$$

$$\times \left[\int_0^{L_2}\int_0^{L_1}[Y_j(x_j) - \overline{Y_j}]\,\psi_p(\boldsymbol{x})dx_1 dx_2 \int_0^{L_2}\int_0^{L_1}[Y_k(x_k') - \overline{Y_k}]\,\psi_p(\boldsymbol{x}')dx_1' dx_2'\right]\delta_{m,n}. \tag{28}$$

The transfer of energy between the two directions is now only possible due to the coupling induced via the stochastic substrate dynamics encapsulated in $\hat{W}_0$. A most natural candidate would be a two-dimensional diffusion process in a periodic potential. We are however faced with the problem that very few results are known about eigenfunctions and eigenvalues when the potential is nontrivial, see e.g., [14]. A way out would be to consider that the coordinate states x_j of the system are not a continuous but a discrete variable, with a discrete periodicity ℓ, ℓ being a positive integer. In this case, one needs to find the eigenfunctions and eigenvalues of the corresponding ℓ by ℓ transition matrix. There is however a much more elegant and interesting model, for which the calculation proceeds without undue effort, and for which the assumption of continuous space does not have to be dropped. We consider the so-called kangaroo process [15], which is a stochastic process where the particle jumps at random times from its current location to a new location. Between jumps, the particle stays put. The distribution of time intervals during which the particles reside in a position before the next jump is Poissonian, in agreement with the Markovian nature

$$P(\Delta t) = \frac{1}{\tau_r}e^{-\Delta t/\tau_r}, \tag{29}$$

where τ_r is the characteristic time between jumps. The kangaroo process has been used in modeling a variety of physical systems, including the well known BGK [18, 19] and Kubo Anderson [15, 20] processes. For a general kangaroo process, τ_r may depend on the position of the particle before the jump. However, in our case detailed balance requires τ_r to be a constant. The new position of the particle after a jump is given by the equilibrium probability distribution

$$P_{\text{eq}}(\boldsymbol{x}) = \langle\boldsymbol{x}|\psi_0\rangle, \tag{30}$$

independently of the position of the particle before the jump. For this process, the operator $\hat{W}_0$ can be written as

$$\hat{W}_0 = -\frac{1 - |\psi_0\rangle\langle\psi_0|}{\tau_r}, \tag{31}$$

where $|\psi_0\rangle$ is the (normalized) ground state of $\hat{W}_0$ with eigenvalue 0 (since $\hat{W}_0|\psi_0\rangle = -(|\psi_0\rangle - |\psi_0\rangle)/\tau_r = 0|\psi_0\rangle$) and all other eigenstates $|\psi_n\rangle$ have eigenvalue $\lambda_n = -1/\tau_r$.

We note that the ground state contribution to the sum in Eq. (28) vanishes, and that all other eigenvalues are equal. Hence using the identity

$$\sum_{p>1}\left[\int_0^{L_2}\int_0^{L_1}f(\boldsymbol{x})\psi_p(\boldsymbol{x})dx_1 dx_2 \int_0^{L_2}\int_0^{L_1}g(\boldsymbol{x})\psi_p(\boldsymbol{x})dx_1' dx_2'\right] = \sum_{p>1}\langle P_{\text{eq}}f|\psi_p\rangle\langle\psi_p|P_{\text{eq}}g\rangle$$

$$= \langle P_{\text{eq}}f|\left(\sum_{p>1}|\psi_p\rangle\langle\psi_p|\right)|P_{\text{eq}}g\rangle = \langle P_{\text{eq}}f|\left(1 - |\psi_0\rangle\langle\psi_0|\right)|P_{\text{eq}}g\rangle$$

$$= \int_0^{L_2}\int_0^{L_1}f(\boldsymbol{x})g(\boldsymbol{x})P_{\text{eq}}(\boldsymbol{x})dx_1 dx_2 - \int_0^{L_2}\int_0^{L_1}f(\boldsymbol{x})P_{\text{eq}}(\boldsymbol{x})dx_1 dx_2 \int_0^{L_2}\int_0^{L_1}g(\boldsymbol{x}')P_{\text{eq}}(\boldsymbol{x}')dx_1' dx_2'$$

$$= \overline{fg} - \overline{f}\,\overline{g} = \overline{\left(f - \overline{f}\right)\left(g - \overline{g}\right)} \tag{32}$$

with $f(\boldsymbol{x}) = Y_j(x_j) - \overline{Y_j}$ and $g(\boldsymbol{x}) = Y_k(x_k) - \overline{Y_k}$ we obtain

$$L^{j,k}_{(m,\zeta),(n,\zeta')} = k_B^{-1}\frac{\omega_n}{2}\overline{[Y_j - \overline{Y_j}]\,[Y_k - \overline{Y_k}]}\frac{\left[\omega_n\tau_r^{-1}\delta_{\zeta,\zeta'} + (-1)^{\delta_{\zeta,c}}\tau_r^{-2}(1-\delta_{\zeta,\zeta'})\right]}{\omega_n^2 + \tau_r^{-2}}\delta_{m,n}, \tag{33}$$

The above explicit expression for the Onsager coefficients still depends on the prefactor involving the correlation function of the Y's. This prefactor quantifies the

strength of the coupling induced by the kangaroo process. It depends on equilibrium probability distribution that defines the kangaroo process. As expected, all the off-diagonal coefficients vanish if $P_{\text{eq}}(\boldsymbol{x})$ can be written as the product of a function of x_1 and a function of x_2, and we do not see work transfer from the driver to the load. For the purpose of illustration we consider a simple situation of coupling induced by having $P_{\text{eq}}(\boldsymbol{x})$ peak strongly along the first diagonal of the x_1/L_1 and x_2/L_2 axes:

$$P_{\text{eq}}(\boldsymbol{x}) = \frac{1 + \alpha\delta\left(\dfrac{x_1}{L_1} - \dfrac{x_2}{L_2}\right)}{L_1 L_2 (1 + \alpha)}. \tag{34}$$

Here, the height of this peak is quantified by the parameter α. In view of the previously cited Curie property, we consider for the displacement functions $Y_j(x_j)$

$$Y_1(x_1) = L_1 \cos\left(\frac{2\pi x_1}{L_1}\right), \quad Y_2(x_2) = L_2 \cos\left(\frac{2\pi x_2}{L_2}\right), \tag{35}$$

together with

$$\mathcal{F}_1(t) = F_1 \cos(\omega_m t), \quad \mathcal{F}_2(t) = F_2 \cos(\omega_n t). \tag{36}$$

The spatial integrals reduce to:

$$\overline{Y_1} = \overline{Y_2} = 0, \qquad \overline{Y_1^2} = \frac{L_1^2}{2}, \tag{37}$$

$$\overline{Y_2^2} = \frac{L_2^2}{2}, \qquad \overline{Y_1 Y_2} = \frac{L_1 L_2 \alpha}{2(1 + \alpha)}, \tag{38}$$

leading to the Onsager coefficients ($j = 1, 2$)

$$L_{(m,c),(n,c)}^{j,j} = k_B^{-1} \frac{(\omega_n L_j)^2}{4} \frac{\tau_r^{-1}}{\omega_n^2 + \tau_r^{-2}} \delta_{m,n}, \tag{39}$$

$$L_{(m,c),(n,c)}^{1,2} = L_{(m,c),(n,c)}^{2,1} = k_B^{-1} \frac{\omega_n^2}{4} \frac{L_1 L_2 \alpha}{(1 + \alpha)} \frac{\tau_r^{-1}}{\omega_n^2 + \tau_r^{-2}} \delta_{m,n}. \tag{40}$$

As expected, the Onsager coefficients are the same for both $Y_1(x_1)$ and $Y_2(x_2)$ sines or cosines (since the coefficients can not depend on the chosen origin of time). However, if one of them is a sine and the other a cosine, we have $L_{(m,c),(n,c)}^{1,2} = L_{(m,c),(n,c)}^{2,1} = 0$. This is a consequence of the strong coupling introduced by the delta function. That is, the kangaroo process defined by the probability density function Eq. (34) does not allow anti-symmetric Onsager coefficients. If $\alpha \to 0$ there is no coupling and the off-diagonal elements again vanish.

We performed simulations of the kangaroo process defined by Eq. (34), modulated by the displacements $Y_j(x_j)$ given in Eq. (35) and the forces $\mathcal{F}_j(t)$ given in Eq. (36). With such a choice, the operator $\hat{W}(\boldsymbol{x}, t)$ becomes

$$\hat{W}(\boldsymbol{x}, t) = \frac{1 - |\psi_{0,\text{ad}}\rangle\langle\psi_{0,\text{ad}}|}{\tau_r}, \tag{41}$$

where $|\psi_{0,\text{ad}}\rangle$ is the ground state for the modulated kangaroo process for a fixed long time, and

$$P_{\text{ad}}(\boldsymbol{x}, t) = \langle\boldsymbol{x}|\psi_{0,\text{ad}}\rangle = \frac{\left[1 + \alpha\delta\left(\dfrac{x_1}{L_1} - \dfrac{x_2}{L_2}\right)\right] e^{-\beta[\mathcal{F}_1(t)Y_1(x_1) + \mathcal{F}_2(t)Y_2(x_2)]}}{L_1 L_2 \left[I_0\left(\beta F_1 \cos(\omega_m t)\right) I_0\left(\beta F_2 \cos(\omega_n t)\right) + \alpha I_0\left(\beta F_1 \cos(\omega_m t) + \beta F_2 \cos(\omega_n t)\right)\right]}. \tag{42}$$

In our simulations, we set $m = n = 1$ in Eq. (42). In addition, we set $L_1 = L_2 = 1$ and $\omega_n = \omega_m = 2\pi$ (i.e., $\tau = 1$). The fluxes where then calculated according to the following algorithm:

1. Choose a random initial point (x, y) where x and y are both uniformly distributed in the range $[0, 1]$.

2. Choose the time interval between jumps according to the exponential distribution $P(\Delta t) = \tau_r e^{\Delta t/\tau_r}$.

3. Calculate the fluxes between t and $t + \Delta t$ and add to

the total flux $J_{\text{tot}}^{(j)} = J_{\text{tot}}^{(j)} + Y_j(x_j)\left[g(t + \Delta t) - g(t)\right]$.

4. Choose a new position according to the probability distribution Eq. (42).

5. Repeat steps 2 to 4 until the time t_{max} is reached. In our simulations, $t_{max} = 5000$.

6. Calculate the average flux $J_{\text{tot}}^{(j)}/t_{\text{max}}$.

7. Repeat steps 1 to 6 N_{samples} times and calculate the average flux. In our simulations, $N_{\text{samples}} = 100$.

In Fig. 1 we successfully compare the predictions of linear response theory for the fluxes with the simulations for three different values of α for weak forces. For strong forces (see inset), the fluxes saturate, as expected. Also, the prediction of linear response theory that the flux $J_c^{(1)}$ (as a function of F_1) does not depend on α holds for strong forces. In Fig. 2, we compare the result of the numerical simulations with the theoretical prediction for the entropy production.
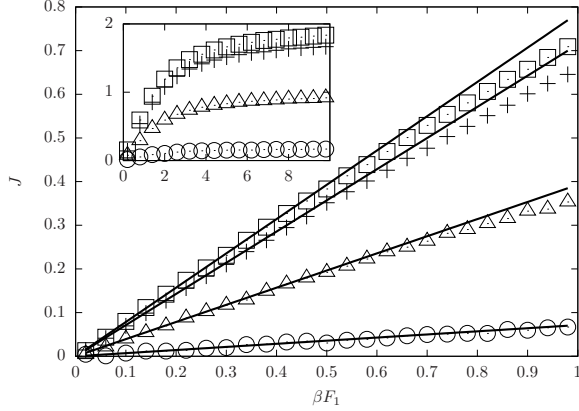

FIG. 1. Flux as a function of βF_1. In the simulations we set $F_2 = 0$ and $\tau_r = \frac{1}{2\pi}$. The lines represent the theoretical results for the linear response regime $J_c^{(j)} = \dfrac{F_1}{T} L_{(1,c),(1,c)}^{1,j}$ with the Onsager coefficients given by Eqs. (39-40), and the symbols represent the results of the numerical simulations for both fluxes: $J_c^{(1)}$ (squares) and $J_c^{(2)}$ for $\alpha = 10.0$ (plus signs), 1.0 (triangles) and 0.1 (circles). In the inset, we show the saturation of the fluxes for strong forces.
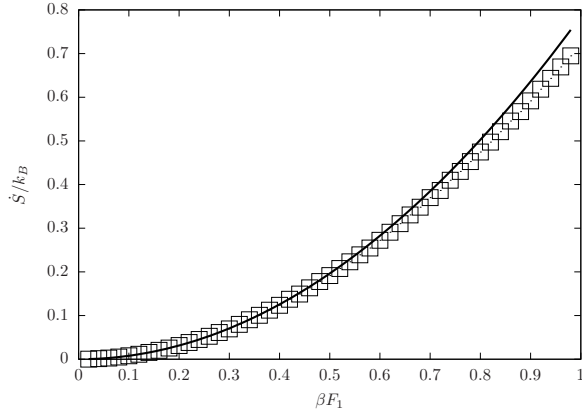

FIG. 2. Entropy production as a function of βF_1. The parameters are the same as in the previous figure, but only a single value of α (0.1) was used because the result is independent of α.

Finally, in Fig. 3 we compare the Onsager coefficients obtained from the numerical simulations with the theoretical predictions as a function of τ_r. The numerical
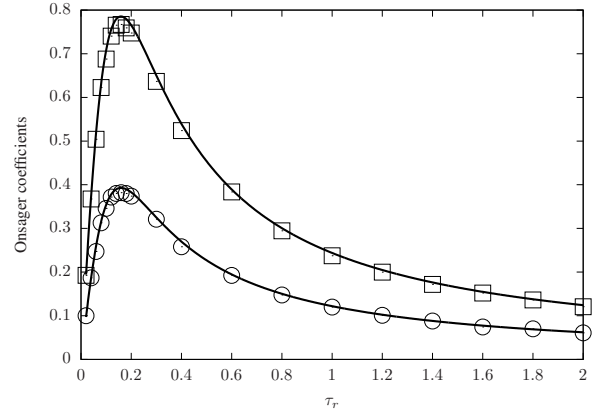

FIG. 3. Onsager coefficients as a function of τ_r. The parameters are the same as in the previous figure. The squares represent the results of the numerical simulations for $L_{(1,c),(1,c)}^{1,1}$ and the circles for $L_{(1,c),(1,c)}^{2,1}$. The lines, are the plots of Eqs. (39) and (40).

simulation results were obtained by linear regression of the fluxes as functions of the force F_1 (for weak forces), for each value of τ_r. Once again, the agreement between the numerical results and the theoretical predictions is notable.

We end this section by stressing that no fitting parameter was required in any of our results.

VI. KANGAROO PROCESS: EFFICIENCY, POWER AND ENTROPY PRODUCTION

It is straightforward to evaluate various quantities of interest from the Onsager coefficients obtained in the previous section. Using the displacement functions Eq. (38) and forces Eq. (36), with $m = n$, one finds for the entropy production per cycle,

$$\begin{aligned}
\dot{S} &= X_c^{(1)} J^{(1)} + X_c^{(2)} J^{(2)} \\
&= \frac{1 + \alpha (1 - \sigma)^2 + \sigma^2}{1 + \alpha} \dot{S}_{MD}.
\end{aligned} \tag{43}$$

For the power $\mathcal{P}$ extracted by the load per cycle,

$$\frac{\mathcal{P}}{T} = -X_c^{(1)} J_c^{(1)} = \frac{\alpha - \sigma (1 + \alpha)}{1 + \alpha} \sigma \dot{S}_{\mathrm{MD}}, \tag{44}$$

and for the efficiency of the machine,

$$\eta = -\frac{X_c^{(1)} J_c^{(1)}}{X_c^{(2)} J_c^{(2)}} = \frac{\alpha - \sigma (1 + \alpha)}{1 + \alpha (1 - \sigma)} \sigma, \tag{45}$$

where

$$\sigma = -\frac{F_1 L_1}{F_2 L_2} \tag{46}$$

and

$$\dot{S}_{\mathrm{MD}}/k_B = \frac{\omega_n^2 \tau_r^{-1} F_2^2 L_2^2}{4 \left(k_B T\right)^2 \left(\omega_n^2 + \tau_r^{-2}\right)}. \qquad (47)$$

To give an idea of the order of magnitude of these quantities, we consider the case $F_2 = 2.0 \ pN$, $F_1 = -1.0 \ pN$, $\tau_r = 1/2\pi \ ms$, $\omega_n = 2\pi \ kHz$, $L_1 = L_2 = 1.0 \ \mu m$, $T = 300.0 \ K$ and $\alpha = 10.0$. The power extracted per cycle is $\mathcal{P} = 0.16 \ pW$ and the entropy production per cycle is $8.6 \times 10^{-4} \ pW/K$.

It is clear from the expression for the power, Eq. (44), and efficiency, Eq. (45), that σ must be positive, since otherwise $\mathcal{P}$ and η would be negative – the power would be injected instead of extracted by the load. Hence, the signs of F_1 and F_2 must be different. What is more, there is a minimum driving force necessary to make the machine work, $\sigma < \alpha/(1 + \alpha)$. In the range $0 \le \sigma \le \alpha/(1+\alpha)$, the entropy production is a monotonically decaying function of σ. Therefore, the maximum entropy production occurs for $\sigma = 0$ ($F_1 = 0$), which gives $\dot{S} = \dot{S}_{\mathrm{MD}}$ defined in Eq. (47). At $\sigma = \alpha/(1 + \alpha)$, the entropy production is a minimum,

$$\dot{S}_{\mathrm{mD}} = \frac{1 + 2\alpha}{(1 + \alpha)^2} \dot{S}_{\mathrm{MD}}. \qquad (48)$$

In both cases (maximum and minimum entropy production), the power extracted from the machine and the efficiency vanish.

The maximum power that can be extracted from the machine can be straightforwardly calculated from Eq. (44) to occur at $\sigma_{\mathrm{MP}} = \alpha/[2(1 + \alpha)]$ and to be

$$\frac{\mathcal{P}_{\mathrm{MP}}}{T} = \frac{\alpha^2}{4 \left(1 + \alpha\right)^2} \dot{S}_{\mathrm{MD}}. \qquad (49)$$

At maximum power, the entropy production is

$$\dot{S}_{\mathrm{MP}} = \frac{4 + 8\alpha + \alpha^2}{4 \left(1 + \alpha\right)^2} \dot{S}_{\mathrm{MD}}, \qquad (50)$$

and the efficiency becomes

$$\eta_{\mathrm{MP}} = \frac{\alpha^2}{4 + 8\alpha + 2\alpha^2}. \qquad (51)$$

In Fig. 4 we show the efficiency as a function of the parameter σ for three values of α. For small α, the predilection of the kangaroo process for the diagonal is weak and so is the coupling between the forces. Consequently, the machine is extremely inefficient. As we increase α, the coupling between the forces becomes stronger and the machine becomes progressively more efficient. It is also clear from the figure that for any given α there is an optimum value of σ for which the efficiency is maximum, which can readily be shown to be

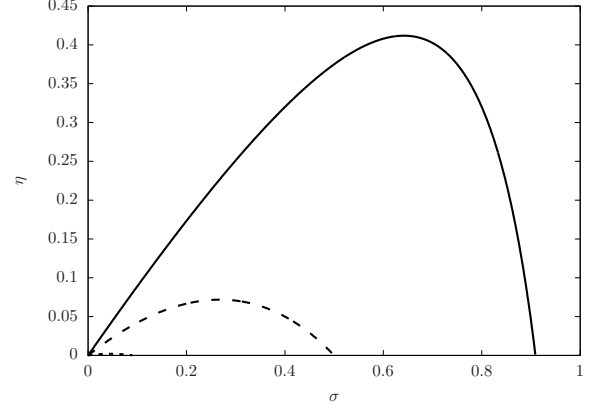$$\sigma_{\mathrm{ME}} = \frac{1 + \alpha - \sqrt{1 + 2\alpha}}{\alpha}, \qquad (52)$$

FIG. 4. Efficiency as a function of the parameter σ for $\alpha = 0.1$ (dotted line), 1.0 (dashed line) and 10.0 (continuous line).

which leads to the maximum efficiency

$$\eta_{\mathrm{ME}} = \frac{\alpha \left(4 + \alpha - 2\sqrt{2\alpha + 1}\right) + 2 - 2\sqrt{2\alpha + 1}}{\alpha^2}, \qquad (53)$$

the power,

$$\begin{aligned} \frac{\mathcal{P}_{\mathrm{ME}}}{T} &= \frac{1 + \alpha - \sqrt{2\alpha + 1}}{\alpha^2(\alpha + 1)} \\ &\times \left[\alpha \left(\sqrt{2\alpha + 1} - 2\right) + \sqrt{2\alpha + 1} - 1\right] \dot{S}_{\mathrm{MD}}, \end{aligned} \qquad (54)$$

and the entropy production,

$$\dot{S}_{\mathrm{ME}} = \frac{2(2\alpha + 1)\left(1 + \alpha - \sqrt{2\alpha + 1}\right)}{\alpha^2(\alpha + 1)} \dot{S}_{\mathrm{MD}}. \qquad (55)$$

It is also worth noting that for $\alpha \to \infty$, the efficiency becomes $\eta_\infty = \sigma$. In this case, the machine may become a perfect machine ($\eta = 1$) for $\sigma = 1$. The power extracted by the load and the entropy production both vanish, that is, the machine becomes reversible. In Fig. 5 we show the maximum efficiency and the efficiency at maximum power (main panel). As α increases and the machine becomes more efficient, the difference between the maximum efficiency and the efficiency at maximum power also increases. For $\alpha \to \infty$, the efficiency at maximum power becomes equal to half of the maximum efficiency. In the inset, we see that the maximum efficiency is reached with smaller values of σ than the ones required to have maximum power.

In Fig. 6, we show the maximum power and the power at maximum efficiency as a function of α. While the maximum power increases monotonically, eventually saturating to $T\dot{S}_{\mathrm{MD}}/4$, at maximum efficiency the power reaches a maximum and slowly decays to zero (as $\alpha \to \infty$).

In Fig. 7, we show the entropy production at maximum efficiency and at maximum power, and the minimum entropy production. Both the minimum entropy production and the entropy production at maximum efficiency vanish proportionally to $1/\alpha$ as $\alpha \to \infty$. At maximum
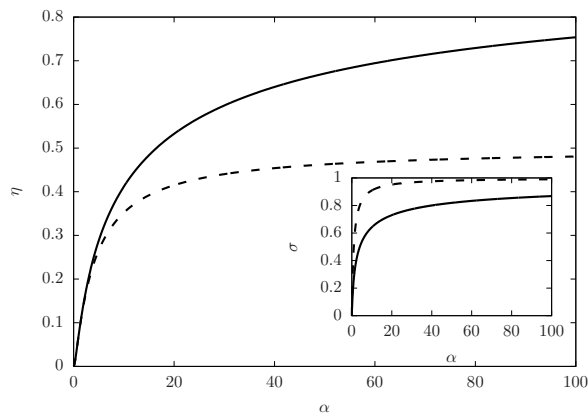
FIG. 5. Maximum efficiency (solid line) and efficiency at maximum power (dashed line) as a function of α (main panel) and σ at maximum efficiency (solid line) and maximum power (dashed line) also as a function of α (inset).
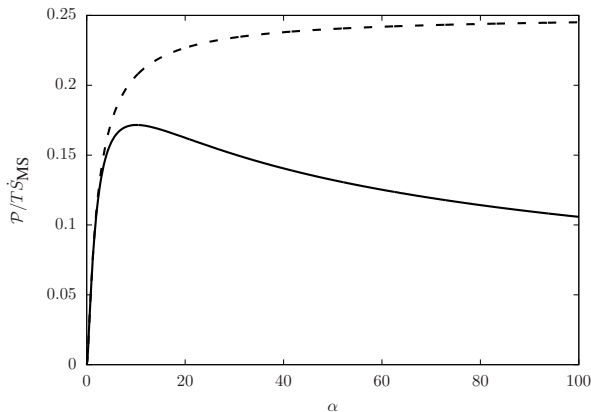

FIG. 6. Power at maximum efficiency (solid line) and maximum power (dashed line) as a function of α.
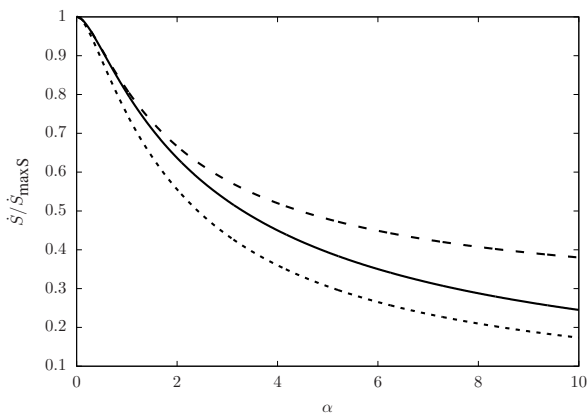

FIG. 7. Entropy production at maximum efficiency (solid line) and at maximum power (large dashed line) and minimum entropy production (small dashed line) as a function of α.

power, however, the entropy production saturates to $1/4$ of its maximum value.

We finally note that the expressions obtained in this section for the entropy production at minimum dissipation Eq. (48), power at maximum power Eq. (49), maximum efficiency Eq. (54) and minimum dissipation (which vanishes), and efficiency at maximum power Eq. (51) and maximum efficiency Eq. (53) are compatible with the general relations obtained in [12].

VII. SUMMARY

In this contribution we have discussed the problem of a particle in a heat bath whose dynamics follows a Markov process, governed by a temporally and spatially periodic transition matrix obeying detailed balance. We obtained expressions for the Onsager coefficients in terms of the eigenvalues of $\hat{W}_0$ and averages over the equilibrium probability density $P_{\mathrm{eq}}(\boldsymbol{x})$ in any dimension. For one-dimensional systems, we recovered the previous results for the Onsager coefficients for a Brownian particle in contact with a heat bath subjected to periodic potentials [13]. We also provided an interesting example of a simple two-dimensional system (the kangaroo process) for which explicit expressions for the Onsager coefficients, entropy production, power and efficiency were obtained. Our results are in very good agreement with numerical simulations and obey exact general relations obtained earlier in [12] for the entropy production, power and efficiency, under different physical circumstances.

Appendix: Onsager coefficients

In order to calculate the Onsager coefficients, we first take the derivative of Eq. (3) with respect to $X_\nu^{(k)}$ in the limit of vanishing modulation,

$$\hat{W}^{(\nu,k)}(\boldsymbol{x},t)P_{\mathrm{eq}}(\boldsymbol{x}) + \hat{W}_0(\boldsymbol{x})P_{\mathrm{ad}}^{(\nu,k)}(\boldsymbol{x},t) = 0, \qquad \text{(A.1)}$$

and use this result to eliminate the dependence of Eq. (22) on $\hat{W}^{(\nu,k)}$,

$$
\begin{aligned}
P^{(\nu,k)}(\boldsymbol{x},t) &= -\int_0^t dt'' e^{\hat{W}_0(\boldsymbol{x})t''}\hat{W}_0(\boldsymbol{x})P_{\mathrm{ad}}^{(\nu,k)}(\boldsymbol{x},t-t'') \\
&= -\int_0^t dt'' \frac{de^{\hat{W}_0(\boldsymbol{x})t''}}{dt''} P_{\mathrm{ad}}^{(\nu,k)}(\boldsymbol{x},t-t'').
\end{aligned}
\qquad \text{(A.2)}
$$

Next, we integrate Eq. (A.2) by parts, so that

$$P^{(\nu,k)}(\boldsymbol{x},t) = -\left. e^{\hat{W}_0(\boldsymbol{x})t''}P_{\mathrm{ad}}^{(\nu,k)}(\boldsymbol{x},t-t'')\right|_0^t - \int_0^t e^{\hat{W}_0(\boldsymbol{x})t''}\dot{P}_{\mathrm{ad}}^{(\nu,k)}(\boldsymbol{x},t-t'')dt''. \qquad \text{(A.3)}$$

Due to the exponential decay of $e^{\hat{W}_0(\boldsymbol{x})t}$ (the eigenvalues of $\hat{W}_0$ cannot be positive, and are zero only in equilibrium [24]), the first term of the integration by parts vanishes at long times, so that

$$P^{(\nu,k)}(\boldsymbol{x},t) = P_{\mathrm{ad}}^{(\nu,k)}(\boldsymbol{x},t) - \int_0^t e^{\hat{W}_0(\boldsymbol{x})t''}\dot{P}_{\mathrm{ad}}^{(\nu,k)}(\boldsymbol{x},t-t'')dt''. \qquad \text{(A.4)}$$

Using this result, the Onsager coefficients can be written as

$$L_{\mu,\nu}^{j,k} = \frac{1}{\tau}\int_0^\tau dt \int_0^{\boldsymbol{L}} d\boldsymbol{x}\, Y_j(x_j)\dot{g}_\mu(t)P_{\mathrm{ad}}^{(\nu,k)}(\boldsymbol{x},t) - \frac{1}{\tau}\int_0^\tau dt \int_0^{\boldsymbol{L}} d\boldsymbol{x}\, Y_j(\boldsymbol{x})\dot{g}_\mu(t)\int_0^t dt' e^{\hat{W}_0 t'}\dot{P}_{\mathrm{ad}}^{(\nu,k)}(\boldsymbol{x},t-t'). \qquad \text{(A.5)}$$

The derivative $P_{\mathrm{ad}}^{(\nu,k)}(\boldsymbol{x},t)$ of the adiabatic probability density $P_{\mathrm{ad}}(\boldsymbol{x},t)$ can be expressed as

$$P_{\mathrm{ad}}^{(\nu,k)}(\boldsymbol{x},t) = -k_B^{-1}Y_k(\boldsymbol{x})g_\nu(t)P_{\mathrm{eq}}(\boldsymbol{x}) + k_B^{-1}P_{\mathrm{eq}}(\boldsymbol{x})g_\nu(t)\int_0^{\boldsymbol{L}} P_{\mathrm{eq}}(\boldsymbol{x}')Y_k(x_k')d\boldsymbol{x}' = k_B^{-1}g_\nu(t)P_{\mathrm{eq}}(\boldsymbol{x})\left[\overline{Y_k} - Y_k(\boldsymbol{x})\right]. \qquad \text{(A.6)}$$

Substituting this expression in the first integral of Eq. (A.5), we have

$$
\begin{aligned}
\frac{1}{\tau}\int_0^\tau dt \int_0^{\boldsymbol{L}} d\boldsymbol{x}\, Y_j(x_j)\dot{g}_\mu(t)P_{\mathrm{ad}}^{(\nu,k)}(\boldsymbol{x},t) &= k_B^{-1}\left[\frac{1}{\tau}\int_0^\tau \dot{g}_\mu(t)g_\nu(t)dt\right]\left[\int_0^{\boldsymbol{L}} Y_j(\boldsymbol{x})\left[\overline{Y_k} - Y_k(\boldsymbol{x})\right]P_{\mathrm{eq}}(\boldsymbol{x})d\boldsymbol{x}\right] \\
&= k_B^{-1}\left[\frac{1}{\tau}\int_0^\tau \dot{g}_\mu(t)g_\nu(t)dt\right]\left[\overline{Y_j}\,\overline{Y_k} - \overline{Y_jY_k}\right].
\end{aligned}
\qquad \text{(A.7)}
$$

The remaining temporal integral vanishes if the frequencies of the Fourier modes μ and ν are different. Even if they are the same, it still vanishes for $\mu = \nu$. Writing $\mu = (m,\zeta)$ and $\nu = (n,\zeta')$, we have

$$
\begin{aligned}
&\frac{1}{\tau}\int_0^\tau dt \int_0^{\boldsymbol{L}} d\boldsymbol{x}\, Y_j(\boldsymbol{x})\dot{g}_\mu(t)P_{\mathrm{ad}}^{(\nu,k)}(\boldsymbol{x},t) \\
&= (-1)^{\delta_{\zeta,c}}k_B^{-1}\frac{\omega_n}{2}\left[\overline{Y_j}\,\overline{Y_k} - \overline{Y_jY_k}\right](1-\delta_{\zeta,\zeta'})\delta_{m,n}.
\end{aligned}
\qquad \text{(A.8)}
$$

We now turn our attention to the remaining integral in Eq. (A.5), which, after substituting the expression for $P_{\mathrm{ad}}^{(\nu,k)}$ given by Eq. (A.6) reads

$$\frac{1}{\tau}\int_0^\tau dt \int_0^{\boldsymbol{L}} d\boldsymbol{x} Y_j(x_j)\dot{g}_\mu(t) \int_0^\infty dt' e^{\hat{W}_0 t'} k_B^{-1}\dot{g}_\nu(t-t')P_{\mathrm{eq}}(\boldsymbol{x})\left(\overline{Y_k} - Y_k(\boldsymbol{x})\right)$$

$$= k_B^{-1}\frac{1}{\tau}\int_0^\tau dt\,\dot{g}_\mu(t)\int_0^\infty dt'\,\dot{g}_\nu(t-t')\int_0^{\boldsymbol{L}} d\boldsymbol{x} Y_j(\boldsymbol{x})e^{\hat{W}_0 t'}P_{\mathrm{eq}}(\boldsymbol{x})\left[\overline{Y_k} - Y_k(\boldsymbol{x})\right]. \quad (A.9)$$

Next, we note that for any real functions $f(\boldsymbol{x})$ and $g(\boldsymbol{x})$ we have that

$$\langle f|e^{\hat{W}_0 t}|g\rangle = \langle f|\left(\sum_p |\psi_p\rangle\langle\psi_p|\right)e^{\hat{W}_0 t}|g\rangle = \sum_p \langle f|\psi_p\rangle\langle\psi_p|e^{\hat{W}_0 t}|g\rangle = \sum_p \langle f|\psi_p\rangle\langle\psi_p|e^{\lambda_p t}|g\rangle$$

$$= \sum_p \left[\int_0^{\boldsymbol{L}} \frac{f(\boldsymbol{x})\psi_p(\boldsymbol{x})}{P_{\mathrm{eq}}(\boldsymbol{x})}d\boldsymbol{x} \int_0^{\boldsymbol{L}} \frac{\psi_p(\boldsymbol{x}')g(\boldsymbol{x}')e^{\lambda_p t}}{P_{\mathrm{eq}}(\boldsymbol{x}')}d\boldsymbol{x}'\right]. \quad (A.10)$$

Identifying the leftmost $Y_j(\boldsymbol{x})$ in the last integral of Eq. (A.9) as $f(\boldsymbol{x})/P_{\mathrm{eq}}(\boldsymbol{x})$ and $P_{\mathrm{eq}}(\boldsymbol{x})\left[\overline{Y_k} - Y_k(\boldsymbol{x})\right]$ as $g(\boldsymbol{x})$, we can write this last integral as,

$$\sum_p \left[\int_0^{\boldsymbol{L}} Y_j(\boldsymbol{x})\psi_p(\boldsymbol{x})d\boldsymbol{x}\right.$$

$$\left. \times \int_0^{\boldsymbol{L}} \psi_p(\boldsymbol{x}')e^{\lambda_p t'}\left[\overline{Y_k} - Y_k(x_k')\right]d\boldsymbol{x}'\right]. \quad (A.11)$$

Combining the results of Eqs. (A.8), (A.9) and (A.11), the Onsager coefficients of Eq. (A.5) with $\mu = (m,\zeta)$ and $\nu = (n,\zeta')$ become

$$L_{(m,\zeta),(n,\zeta')}^{j,k} = (-1)^{\delta_{\zeta,c}}k_B^{-1}\frac{\omega_n}{2}\left(\overline{Y_j}\,\overline{Y_k} - \overline{Y_j Y_k}\right)(1-\delta_{\zeta,\zeta'})\delta_{m,n} - k_B^{-1}\sum_p \frac{1}{\tau}\int_0^\tau dt\,\dot{g}_\mu(t)\int_0^\infty dt' e^{\lambda_p t'}\dot{g}_\nu(t-t')$$

$$\times \int_0^{\boldsymbol{L}} Y_j(\boldsymbol{x})\psi_p(\boldsymbol{x})d\boldsymbol{x} \times \int_0^{\boldsymbol{L}} \psi_p(\boldsymbol{x}')\left[\overline{Y_k} - Y_k(x_k')\right]d\boldsymbol{x}'. \quad (A.12)$$

We rewrite this expression in a more symmetrical form noticing that

$$\int_0^{\boldsymbol{L}} \psi_p(\boldsymbol{x}')\overline{Y_k}d\boldsymbol{x}' = \overline{Y_k}\int_0^L \frac{\psi_p(\boldsymbol{x}')P_{\mathrm{eq}}(\boldsymbol{x}')}{P_{\mathrm{eq}}(\boldsymbol{x}')}d\boldsymbol{x}' \quad (A.13)$$

$$= \overline{Y_k}\langle\psi_p|P_{\mathrm{eq}}\rangle.$$

Since $|P_{\mathrm{eq}}\rangle = |\psi_0\rangle$, we have that this integral is zero for $j > 0$. For $j = 0$, the last integral in Eq. (A.12) yields

$$\int_0^L P_{\mathrm{eq}}(x')\left[\overline{Y_k} - Y_k(x')\right]dx' = \overline{Y_k} - \overline{Y_k} = 0 \quad (A.14)$$

so we can write the Onsager coefficients as

$$L_{(m,\zeta),(n,\zeta')}^{j,k} = -(-1)^{\delta_{\zeta,c}}k_B^{-1}\frac{\omega_n}{2}\overline{\left[Y_j - \overline{Y_j}\right]\left[Y_k - \overline{Y_k}\right]}(1-\delta_{\zeta,\zeta'})\delta_{m,n}$$

$$+ k_B^{-1}\sum_p \frac{1}{\tau}\int_0^\tau dt\,\dot{g}_\mu(t)\int_0^\infty dt' e^{\lambda_p t'}\dot{g}_\nu(t-t')\left[\int_0^{\boldsymbol{L}}\left[Y_j(\boldsymbol{x}) - \overline{Y_j}\right]\psi_p(\boldsymbol{x})d\boldsymbol{x}\int_0^{\boldsymbol{L}}\left[Y_k(\boldsymbol{x}') - \overline{Y_k}\right]\psi_p(\boldsymbol{x})d\boldsymbol{x}'\right]. \quad (A.15)$$

To actually perform the integral over t' we need to distinguish between cosine and sine Fourier modes. Most of

the remaining integrals involve simply exponentials and sines or cosines. After some tedious steps we finally arrive at Eq. (23) for the Onsager coefficients.

[1] S. Schmiedl and U Seifert, Europhys. Lett. 81, 20003 (2008).

[2] Y. Izumida and K. Okuda, Phys. Rev. E 80, 021121 (2009).

[3] Y. Izumida and K. Okuda, Eur. Phys. J. B 77, 499 (2010).

[4] M. Esposito, R. Kawai, K. Lindenberg and C. Van den Broeck, Phys. Rev. E 81, 041106 (2010).

[5] Y. Izumida and K. Okuda, Europhys. Lett. 97, 10004 (2012).

[6] Y. Izumida and K. Okuda, New J. Phys. 17, 085011 (2015).

[7] K. Brandner, K. Saito and U. Seifert, Phys. Rev. X 5 031019 (2015).

[8] K. Proesmans and C. Van den Broeck, Phys. Rev. Lett. 115, 090601 (2015).

[9] K. Proesmans, B. Cleuren and C. Van den Broeck, J. Stat. Mech. 023202 (2016).

[10] G. Benenti, K. Saito, and G. Casati, Phys. Rev. Lett. 106, 230602 (2011).

[11] K. Brandner, K. Saito, and U. Seifert, Phys. Rev. Lett. 110, 070603 (2013).

[12] K. Proesmans, B. Cleuren, and C. Van den Broeck, Phys. Rev. Lett. 116, 220601 (2016).

[13] A. Rosas, C. Van den Broeck, and K. Lindenberg, submitted.

[14] Kac, Mark. "Can One Hear the Shape of a Drum?" The American Mathematical Monthly 73, 1 (1966).

[15] A. Brissaud and U. Frisch, J. Math. Phys. 15, 524 (1974).

[16] S. Herrmann and D. Landon, Stoch. Dyn. 15, 1550022 (2015).

[17] B. Alberts, A. Johnson, J. Lewis, D. Morgan, M. Raff, K. Roberts, and P. Walter, *Molecular Biology of the Cell*, 6thed. (Garland Science, New York, 2014).

[18] P. L. Bhatnagar, E. P. Gross, and M. Krook, Phys. Rev. 94, 511 (1954).

[19] P. Welander, Ark. Fys. 7, 507 (1954)

[20] P.W. Anderson, J. Phys. Soc. Jpn. 9, 316 (1954); R. Kubo, ibid. 9, 935 (1954).

[21] K. Sekimoto, J. Phys. Soc. Jpn., 66, 1234 (1997); Prog. Theor. Phys. Supp. 130, 17, (1998).

[22] I. Prigogine, *Introduction to Thermodynamics of Irreversible Processes* (Interscience Publishers, New York, 1961).

[23] S. R. De Groot and P. Mazur, *Non-equilibrium Thermodynamics* pp. 6183 (North-Holland Publ. Co., Amsterdam, 1962).

[24] H. Risken, *The Fokker-Plank Equation*, (Springer-Verlag, 2nd edition, 1989).